Influence of Torsional Anharmonicity on the Reactions of Methyl Butanoate with Hydroperoxyl Radical

Qinghui Meng[1,2], Lidong Zhang[2], Qinxue Chen[1], Yicheng Chi[1] and Peng Zhang[1,*]

1. Department of Mechanical Engineering, The Hong Kong Polytechnic University, Hong Kong

2. National Synchrotron Radiation Laboratory, University of Science and Technology of China, Hefei 230029, Anhui, P. R. China

Abstract: An ab initio chemical kinetics study of the reactions of methyl butanoate (MB) with hydroperoxyl radical (HO_2) is presented in this paper. Particular interest is placed on determining the influences of torsional anharmonicity and addition reaction on the rate constants of hydrogen abstraction reactions. Stationary points on the potential energy surface of MB + HO_2 are calculated at the level of QCISD(T)/CBS//B3LYP/6-311++G(d,p). The transition state theory (TST) is used to calculate the high-pressure limit rate constants of the hydrogen abstraction reactions over a board range of temperature (500-2000K). Anharmonicity of low-frequency torsional modes is considered in the rate calculations by using the one-dimensional hindered rotor approximation and the internal-coordinate multi-structural approximation. The calculated rate constants are compared with the available data from the literature and observed discrepancies are analyzed in detail. An energetically lowest-lying addition reaction with subsequent isomerization and decomposition reactions are identified on the potential energy surface. The multiple-well Master equation analysis shows that these reactions have a secondary influence on the rate constants in the temperature range of interest.

1. Introduction

As an important non-petroleum-based alternative fuel, biodiesel has gained extensive attention in recent years for its potential merits in reducing greenhouse gases and NOx emissions[1, 2]. Efforts have been made for the development of biodiesel mechanism [3, 4]. Methyl butanoate (MB, $C_5H_{10}O_2$) has been widely used as a prototype molecule for understanding chemical kinetics of biodiesel combustion. A number of detailed chemical reaction mechanisms for MB combustion have been proposed and validated [5-9]. Regardless of the success of these mechanisms in modeling key combustion parameters under various experimental conditions, discrepancies between model predictions and experimental data were observed and attributed to a few typical chain-branching and chain-propagation reactions. The reactions of MB with HO_2 are of particular importance in relatively low-temperature and high-pressure environments. For example, Liu et al.[10] found that ignition delays are very sensitive to the rate constants of MB + HO_2 at the temperature of 1300K, at the pressures of 20 and 40 atm, and at the global equivalence ratio of two, which are representative of conditions in realistic compression-ignition engines.

No direct experimental measurement has been conducted for the rate constants of MB + HO_2 and only a few theoretical studies were attempted. Fisher et al.[6] utilized a bond additivity method to estimate the rate constants, which were subsequently modified by Metcalfe el al.[8], Walton et al.[9] and Dooley et al.[5] to fit the data from various experimental facilities. Liu et al.[10] generated preliminary rate rules for MB + HO_2 by utilizing analogies from experimental and theoretical studies on alkanes. Recently, Mendes et al.[11] used a theoretical method of CCSD(T)/cc-pVTZ//MP2/6-311++G(d,p) to study the hydrogen abstraction reactions of MB by HO_2. In their study, the low-frequency torsional modes were treated as one-dimensional hindered rotors.

In a similar system of MB + OH studied by Zhang et al.[12], intramolecular hydrogen bonds were found to stabilize the transition state structures and so as to yield the lowest-energy torsional states. One-dimensional hindered rotor (1D–HR for short hereinafter) approximation was used to

produce the rate constants that are in good agreement with Le Calve et al.'s[13] experimental measurements. In the study of Yang et al.[14], the predicted rate constants for methyl acetate (MA) + HO_2 using the 1D–HR method are about 5–10 times smaller than the experimentally determined values. They attributed the large discrepancy to the complex transition state structures, to which the 1D–HR method may be inaccurate. Similar observations were also made in the theoretical studies of Mendes et al.[11] for ketones + HO_2 and of Klippenstein et al.[15] for methanol + HO_2. Consequently, we expected that the MB+HO_2 system may exhibit the similar behavior because the longer carbon chain of MB and the emergent intramolecular hydrogen bonds may result in even more complex transition state structures.

Noteworthy progress in including torsional anharmonicity in thermochemical and chemical kinetic calculations on complex molecules has been made in recent years [16-21]. Notably, the internal-coordinate multi-structure (MS for short hereinafter) approximation was proposed to remedy the deficiency of the 1D–HR method in dealing with strongly coupled torsional modes. The method has been applied to similar systems such as 1-butanol + HO_2 by Seal et al.[16], n-butanol + HO_2 by Alecu et al.[22], and butanal + HO_2 by Zheng et al.[17]. Several worthy observations have been made by the authors to the MS method through the course of the present study. First, a significantly large amount of electronic structure calculations must be done to search all the possible torsional states of concerned species. For example, 262 conformational structures of the transition state were identified for the hydrogen abstraction from Carbon-3 of 1-butanol by HO_2[16], 188 for the hydrogen abstraction from Carbon-1 of n-butanol by HO_2[16], and 254 for the transition states of butanal + HO_2[17]. Second, the multi-structural anharmonicity is sensitive to the number of conformers mainly because the conformational-rovibrational partition function calculated in the MS method is a weighted summation of those from every structure [23]. Third, the predicted rate constants (equivalently, partition functions, given the same activation energy) by the MS method are usually larger than those neglecting the multiple-structural anharmonicity by one order of magnitude or even more.

Rate constants obtained by the MS method were occasionally compared with those by the 1D–HR method. Mendes et al. [11] found that the rate constants for the hydrogen abstractions from the α and γ sites of n-butanol are similar to those reported by Alecu et al.[22]. Yang et al.[14] found that multiplying a correction factor of 46 at 1000K, recommended by the same study of n-butanol + HO_2, to the rate constants of MA + HO_2 in their kinetics modeling results in a substantially better agreement with the experiment data. Nevertheless, the detailed comparison between the MS method and the 1D–HR method has not been attempted.

Based on the above considerations, we formulated the present theoretical study of the reactions between MB and HO_2 with emphasis on clarifying the role of torsional anharmonicity in affecting the rate constants. Particularly, the rate constants from the 1D–HR method were thoroughly compared with those from the MS method. Moreover, previously ignored addition reactions of HO_2 to MB followed by a large number of isomerization and β-scission reactions were identified and analyzed for their kinetic significance.

2. Theoretical Methods

2.1 Electronic structure calculation methods

Density functional theory (DFT) employing the B3LYP functional with the 6-311++G(d,p) basis set[24] was used for all the geometry optimization and vibrational frequency calculations of the stationary points on the MB + HO_2 potential energy surface. Transition states were identified through the intrinsic reaction coordinate (IRC) calculation by examining the connections of each saddle point to its local minima. The vibrational frequencies were not scaled by the common factor of 0.95-0.99 since it is believed to not cause significant influence on the present rate calculations [12]. The high-level single point energies were obtained by the QCISD(T)/CBS method expressed as follows:

$$\mathrm{E[QCISD(T)/CBS]} = \mathrm{E[QCISD(T)/CBS]_{DZ\rightarrow TZ}} + \{\mathrm{E[MP2/CBS]_{TZ\rightarrow QZ}} - \mathrm{E[MP2/CBS]_{DZ\rightarrow TZ}}\} \quad (1)$$

This QCISD(T)/CBS method has been examined by Zhang et al. [25] for alkyl esters and proved to be an efficient and accurate method for high-level energy estimation. All the zero-point energy corrections were predicted at the B3LYP/6-311++G(d,p) level of theory. Natural bond order (NBO) analysis was employed to evaluate the bond orders of the intramolecular hydrogen bonds. No significant spin contamination was found for all the radicals in the present study, in consistent with our previous observation [12]. All the calculations were performed with the Gaussian 09 program package [26].

2.2 Kinetic theory

For the hydrogen abstraction reactions of MB + HO_2, a barrierless reaction channel was identified to connect a van der Waals (vdW) complex that goes through saddle points to form products. Since the energies of all transition states are higher than the energy of MB +HO_2, the influence of the barrierless reaction channel is negligible in the concerned temperature range above 500K. Thus, transition state theory (TST) with an asymmetric Eckart tunneling correction [27] and the rigid-rotor harmonic-oscillator (RRHO) approximation for all internal degrees of freedom except torsional ones was employed for all the reactions. It should be noted that the torsional modes are strongly coupled in the transition states involving hydrogen bonds. In order to treat the torsional modes soundly, the 1D-HR and the MS methods were employed to deal with the torsional anharmonicity for comparison. The pressure-dependent rate calculations were performed by using the multiple-well Master equation analysis[28]. All the rate calculations were performed by using the Variflex program suite.

2.2.1 The 1D-HR approximations

In the first method, the low-frequency torsional modes were treated as 1D–HRs using Pitzer-Gwinn-like approximations and the $I^{(2,3)}$ moments of inertia[29]. The hindrance potentials were obtained by using the relaxed potential energy surface scan with the increment of 12 degrees at the

B3LYP/6-311++G(d,p) level. Fourier-series-like fitting was conducted to fit the force constant at the global minimum and the energies of the local extrema to reproduce the hindrance potentials as follows:

$$f(x) = a_0 + \sum_{m=1}^{M} a_m \cos(mx) + \sum_{n=1}^{N} b_n \sin(nx) \quad (2)$$

where x is the dihedral corresponding to a torsional mode, M and N are the numbers of cosine and sine functions used in the fitting, respectively.

2.2.2 The MS method

The MS method employed in this work was proposed by Truhlar and coworkers and has been sufficiently described in Ref [16, 18, 19]. For a brief summary, the conformational-rovibrational partition function of torsional modes without assuming either the separability or the one-to-one correspondence to specific normal modes were calculated by considering J distinguishable structures of conformational minima, j=1, 2, ..., J, and including torsional modes τ=1, 2, ... ,t in each structure as follows:

$$Q_{con-rovib} = \sum_{j=1}^{J} Q_j^{rot} \exp(-\beta U_j) Q_j^{HO} Z_j \prod_{\tau=1}^{t} f_{j,\tau} \quad (4)$$

where Q_j^{rot}, U_j and Q_j^{HO} are the rotational partition function, the relative energy with respect to a reference structure, and the harmonic oscillator vibrational partition function of the j-th structure, respectively. The internal-coordinate torsional anharmonicity function $f_{j,\tau}$, together with Z_j that is a factor designed to ensure the correct high-temperature limit, accounts for the presence of the torsional mode τ in the j-th structure. Without assuming separable torsional modes and assigning specific normal modes to them, the MS method can be used to address the influence of strongly coupled torsional modes.

Since the partition function is sensitive to the number of conformational structures, identifying all the distinguishable torsional states is the most challenging and time-consuming procedure in the application of the MS method. Basically, one should carry out a search of all conformational

structures that are accessible by internal rotations of an initial structure (usually the lowest-energy torsional state), and analyze all the optimized structures to remove identical ones, and finally take into account the symmetry of each structure to include its enantiomer that is accessible by internal rotation. Special attentions should be given to some cases that have been discussed in Ref. [19]. All the calculations employing the MS method were performed by using the MSTor program package[18].

2.2.3 Pressure-dependent kinetic theory

As will be shown in the section, the addition reactions of MB+HO_2 involves multiple wells interconnected with each other and with multiple products. The pressure-dependent kinetic parameters were obtained by solving the time-dependent multi-well Master equation. For the average downward energy transfer, its energy transfer probability was approximated by using one single-exponential-down model: $\Delta E_{down} = 200(T/300)^{0.85}$. The Lenard-Jones parameters of MB was σ = 5.85 A˚ and ε = 227 cm^{-1}, which has been validated in the related studies of MB [30].

3. Results and Discussion

3.1 Potential Energy Surfaces

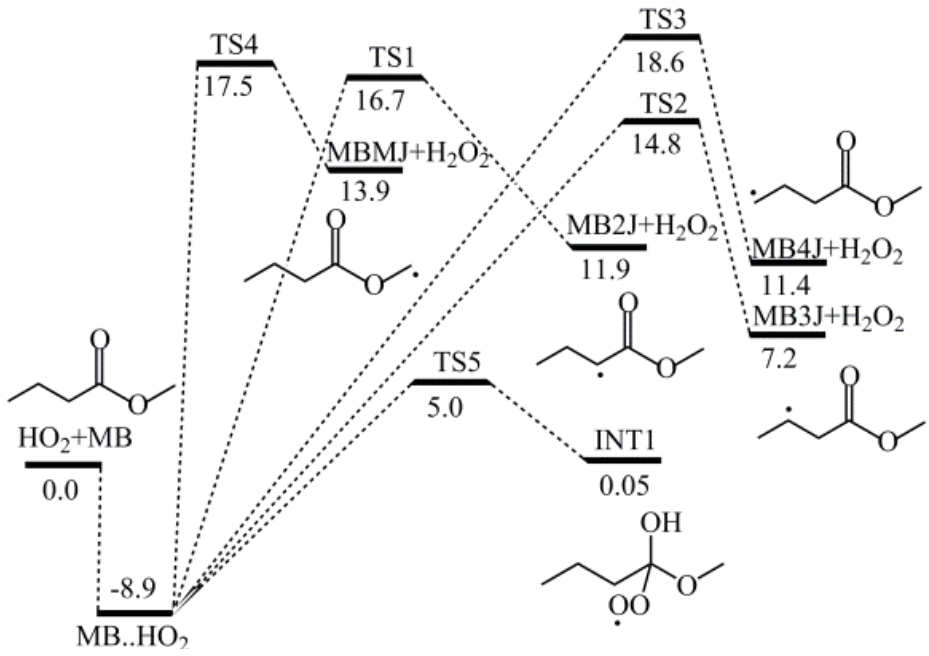

Figure 1. PES of the hydrogen abstraction reactions and the addition reaction of MB + HO_2 at the QCISD(T)/CBS//B3LYP/6-311++G(d,p) level. Unit: kcal/mol.

Among many reactions identified on the potential energy surface (PES) of MB + HO_2, only those energetically favorable and therefore kinetically significant are shown in Figure 1 for simplicity and clarity. The most important bimolecular reactions are

$$MB+HO_2 \xrightarrow{TS1} CH_3CH_2C\cdot HC(O)OCH_3+H_2O_2 \quad (R1)$$

$$MB+HO_2 \xrightarrow{TS2} CH_3C\cdot H\ CH_2C(O)OCH_3+H_2O_2 \quad (R2)$$

$$MB+HO_2 \xrightarrow{TS3} C\cdot H_2CH_2CH_2C(O)OCH_3+H_2O_2 \quad (R3)$$

$$MB+HO_2 \xrightarrow{TS4} CH_3CH_2CH_2C(O)OC\cdot H_2+H_2O_2 \quad (R4)$$

which correspond to the hydrogen abstractions from the α, β, γ sites of the carbon chain and from the α' site of the methyl group, respectively. In the following text, the MB radicals are denoted by MB2J, MB3J, MB4J and MBMJ, respectively, being in consistent with the nomenclature used in the previous studies [3, 30]. A pre-reaction vdW complex MB...HO_2 was also identified to be 8.9 kcal/mol lower than the reactants and is kinetically unimportant at sufficiently high temperature, say, above 500K [11, 12].

The lowest-energy torsional states for all the stationary points on the PES were systematically determined by scanning the PES for all the internal rotational degrees of freedom and subsequently selecting the global minima for further refined optimization. We note that TS1 leading to MB2J has a higher barrier than that of TS2 leading to MB3J, implying that the latter is kinetically more important at low temperatures. This seems to contradict the rule of thumb that the α-hydrogen can be more readily abstracted than the β-hydrogen. The underlying physics is that the hydrogen bond involved in TS2 is stronger than that in TS1 and thereby makes TS2 more energetically stable than TS1.

Addition reactions of HO_2 to MB were always neglected in the previous studies, which implicitly assume they are energetically unfavorable. In the present study, an energetically lowest-lying addition reaction channel via TS5 to form an intermediate complex INT1 was identified on the

PES, as shown in Figure 1. The barrier height of TS5 is as low as 5.0 kcal/mol so that R5 may be the dominant MB+HO_2 channel at sufficiently low temperatures. INT1 can further isomerize to INT6-INT9 followed by a number of isomerization and β-scission reactions shown in Figures S1-S5 of Supplementary Material I. However, the energy barriers of these reactions are too high compared with R1-R4 to be energetically favorable.

In order to elaborate the above analysis, two competitive reaction pathways in addition reactions are given by

$$MB+HO_2 \xrightarrow{TS5} INT1 \xrightarrow{TS6} INT6 \xrightarrow{TS6-1} CH_3CH_2CH_2COOH+OH+CH_2O \quad (R5)$$

$$MB+HO_2 \xrightarrow{TS5} INT1 \xrightarrow{TS8} INT8 \xrightarrow{TS8-4} CH_2(OH)OOCH_3+OH+C_3H_6 \quad (R6)$$

INT1 can isomerize to INT6 via TS6 of 21.4 kcal/mol and in turn decompose to the products consisting of butanoic acid, formaldehyde and OH via TS6-1 of 29.8 kcal/mol, as shown in Figure 2. Similarly, INT1 goes through TS8 of 22.5 kcal/mol to form the INT8, which decomposes to products through the transition state TS8-4 of the 28.2 kcal/mol. In addition, INT1 can also isomerize to INT7 and INT9 via TS7 and TS9, respectively, which are energetically comparable with TS6. The subsequent isomerization and β-scission reactions of INT6-INT9 are shown in Figures S1-S3 of Supplementary Material I. However, the energy barriers of these reactions are too high compared with R1-R4 to be energetically favorable. Moreover, it is found that the energy barrier of the reverse reaction of R5 is 4.95 kcal/mol, which is significantly smaller than those of the isomerization reactions of INT1 to INT6-INT9. Consequently, HO_2 may tend to be added to MB for form INT1 at relatively low temperatures but INT1 may equilibrate with the reactants at higher temperatures, rendering the subsequent reactions to be kinetically unfavorable compared with R1-R4. This inference will be confirmed in Section 3. 5 by using the multiple-well master equation analysis.

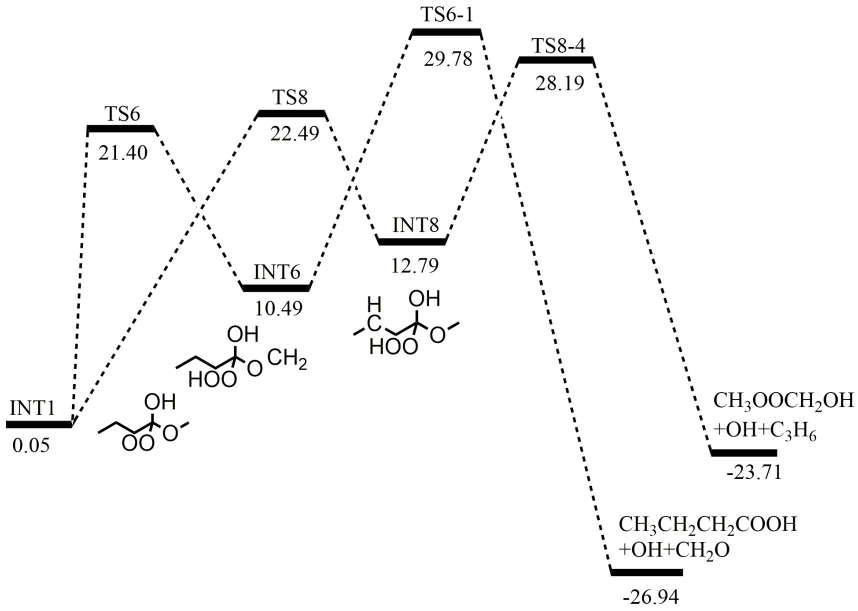

Figure 2. PES of the subsequent reactions of INT1 at the QCISD(T)/CBS//B3LYP/6-311++G(d,p) level. Unit: kcal/mol.

3.2 Lowest-energy conformers

The above finding that hydrogen bonding stabilizes transition state structure leaded us to search all the lowest-energy torsional states of TS1-TS4 either with a hydrogen bond (denoted by "w/ HB" for short hereinafter) or without a hydrogen bond (denoted by "w/o HB" for short hereinafter), as shown in Figure 3. The calculated barrier heights of R1-R4 are listed in Table 1 for comparison with those obtained by Mendes et al. [11] at the level of CCSD(T)/cc-pVTZ//MP2/6-311++G(d,p). The present results show that the barrier heights of R1-R4 follow the orders of R2 < R3 < R1 < R4 (w/HB) and R1 < R2 < R4 < R3 (w/o HB). Mende et al.'s results show R2 < R1 < R4 < R3, where the structures with or without hydrogen bonds are not treated differently. It is seen that TS2 (w/ HB) and TS2 (w/o HB) are energetically different by 2.6 kcal/mol, because of the strongest hydrogen bond (NBO=0.0054) in TS2 (w/ HB), while TS1 (w/ HB) is only 0.3 kcal/mol higher and that of TS1 (w/o HB). A possible explanation is that the energetic stabilization of the nearly weakest hydrogen bond (NBO=0.0025) in TS1(w/ HB) is insufficient to overcome the energy increase by the formation of the tight seven-member ring structure. The structurally distinct albeit energetically similar torsional

states either with or without hydrogen bonds should be considered for their different contributions to the rate constants.

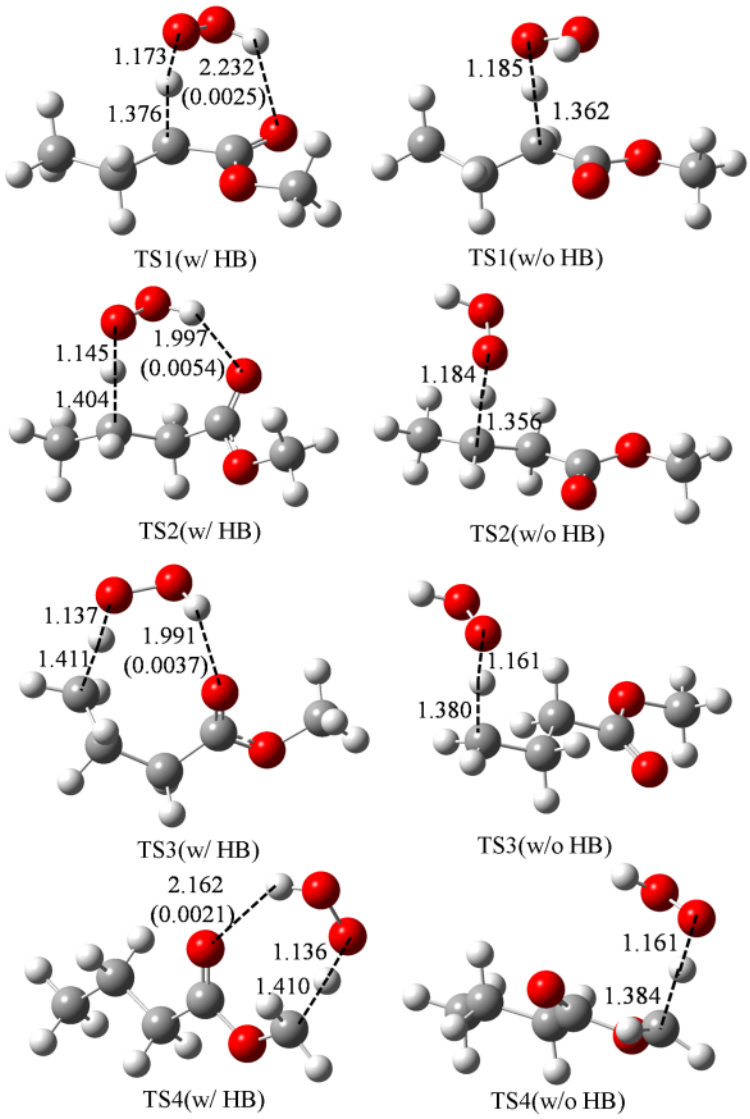

Figure 3. Molecular Structures of the lowest-energy torsional states of TS1-TS4 with a hydrogen bond (w/ HB) or without a hydrogen bond (w/o HB). NBOs are given in the brackets. Unit: Angstrom

Reactions	Present work		Reference
	w/ HB	w/o HB	[8]
MB + HO_2→MB2J + H_2O_2 (R1)	17.0	16.7	15.9 *
MB + HO_2→MB3J + H_2O_2 (R2)	14.8	17.4	15.5 *
MB + HO_2→MB4J + H_2O_2 (R3)	15.6	19.6	19.7 **

MB + HO_2→MBMJ + H_2O_2 (R4)	17.5	18.5	18.5 **

Table 1. Calculated barrier heights for R1-R4 of MB+HO_2. Unit: kcal/mol. * the TS structures have hydrogen bonds; ** the TS structures do not have hydrogen bonds

3.3 Torsional Anharmonicity

In the present study, relaxed scans of torsional potential for all the possible torsional modes in MB and TS1-TS4 were conducted with a 12-degree increment in dihedral angle for totally 360 degrees. The strongly coupled torsional modes may make the 1D torsional potential different for the scan of the same dihedral of different structures with hydrogen bond and without hydrogen bond. Thus, the lowest conformer with hydrogen bond and those without hydrogen bond were separately scanned and fitted, as presented in Supporting Material II.

In the present calculation employing the MS method, the numbers of identified distinguishable conformers are 6 for MB; 78, 46, 78 and 88 for the hydrogen abstraction at the α, β, γ and α' positions, respectively. A direct validation of these results is difficult but similar results have been obtained by Zheng et al.[17] for butanal+HO_2, in which 7 structures were identified for butanal, and 60, 72, 76 and 46 for the hydrogen abstraction at the α, β, γ and carbonyl positions, respectively. The detailed information for the 296 structures, together with all the key parameters required by the MS method, is given in Supplementary Material III.

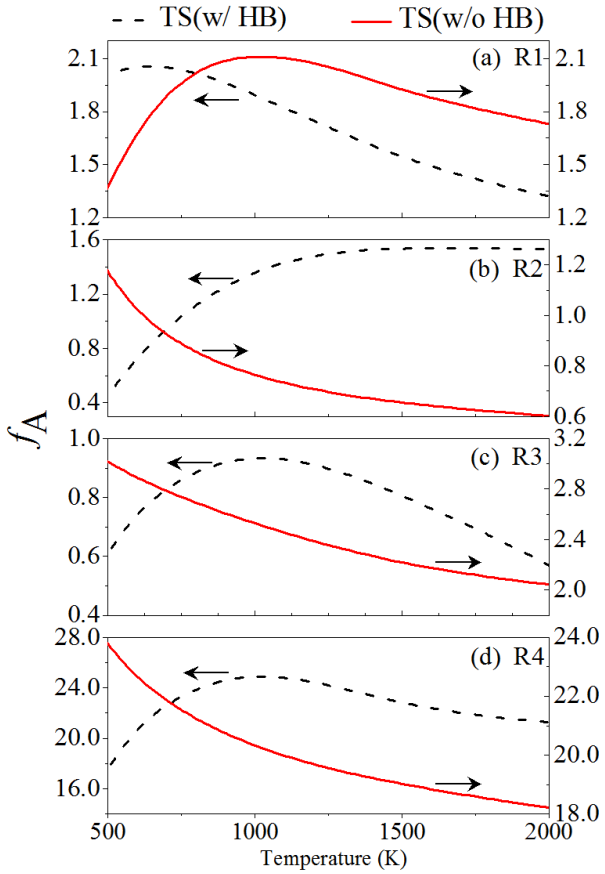

Figure 4. The non-dimensional ratios of the pre-exponential A-factors for the comparison between the 1D–HR and the MS methods.

To compare the 1D–HR and the MS methods, we defined a non-dimensional ratio f_A by

$$f_A = \frac{A_{MS}}{A_{1D-HR}} = \frac{\left(\frac{Q^{\neq}}{Q^R}\right)_{MS}}{\left(\frac{Q^{\neq}}{Q^R}\right)_{1D-HR}} \quad (5)$$

where A_{MS} and $A_{1D\text{-}HR}$, in an analogy with the pre-exponential "A-factor", are the ratios of the total partition functions of the transition state to that of the reactants, calculated by the MS and the 1D–HR methods, respectively. This ratio was calculated separately for each transition state structures with and without hydrogen bond, and it therefore can reflect their different entropies.

The calculated ratios f_A for R1-R4 are shown in Figure 4. It is seen that f_A of R1 (either with or without hydrogen bounding) is within 1 to 2 for TS1, indicating that the 1D–HR method can produce similar results as the MS method for the hydrogen abstraction reaction from the α-site of MB. Similar observation has been made by Mendes et al. [11] for n-butanol + HO_2.

The largest discrepancies between the MS and the 1D–HR predictions were found for R4 as f_A is as large as 15-28 indicating that the MS predictions for these cases are significantly larger than the 1D-HR predictions. Since the MS method considers all the torsional states including those that are strongly coupled and therefore not accessible by internal rotations from these transition states tightened hydrogen bonds, the f_A increases if the strongly-coupled modes are treated as harmonic oscillators by the 1D–HR method.

It is found that f_A can be as small as about 0.5 for TS2(w/o HB) and TS3(w/o HB), indicating that the 1D–HR predictions for these cases are actually 2 times larger than the MS predictions. This is because a few harmonic modes with very low frequencies appear in the loose structures of transition states. The uncertainty of these low-frequency modes significantly affects the calculated rate constants to be discussed in the following section.

3.3 High-pressure Rate Constants of R1-R4

Figure 5 shows the predicted high-pressure rate constants of R1-R4 based on the 1D–HR and MS methods together with the previous theoretical data from Mendes et al. [11], in which the details of their 1D–HR treatments are unavailable. Overall, the rate constants based on TS(w/o HB) agree well with those based on TS(w/ HB) at high temperatures, although the formers have higher energy barriers. This result is in consistent with the observation that $A_{1D\text{-}HR}$ of TS(w/o HB) is generally comparable with that of TS(w/ HB).

For R1 shown in Figure 5(a), the rate constants calculated by the 1D–HR method with TS1(w/o HB) are in good agreement with those by the MS method, because they have very close barrier heights and "A-factors". In addition, the discrepancy of rate constants for R1 between the 1D-HR(w/ HB) and Mendes et al. have been observed at low temperatures, because the TS1(w/ HB) of Mendes et al. [11] is lower than that of TS1(w/ HB) in the present work by 1.1 kcal/mol.

For R2 shown in Figure 5(b), the good agreement of the rate constant by the 1D–HR method with TS2(w/ HB) and that of TS2(w/ HB) of Mendes et al. [11] was observed due to their similar energy barriers. Because of the loose structure of TS2(w/o HB) and higher entropy change, the rate constant by 1D-HR(w/o HB) is slightly higher than that by 1D-HR(w/o HB).

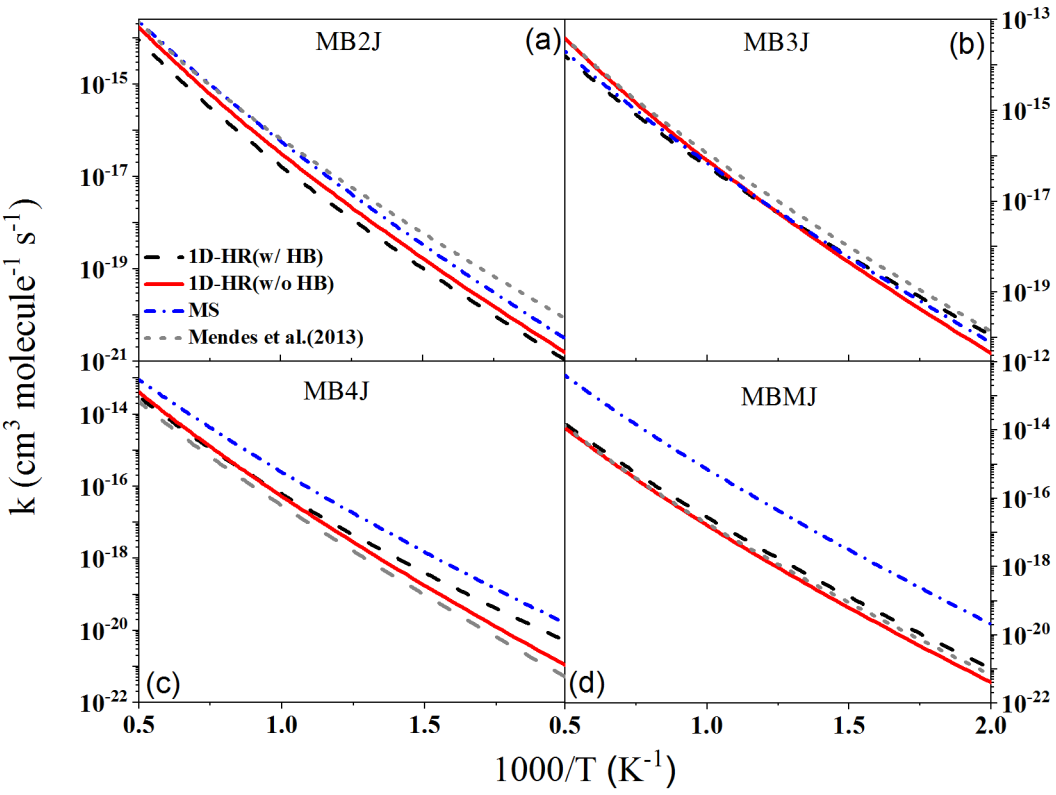

Figure 5. High-pressure rate constants of R1-R4 by the 1D–HR and MS methods.

For R3 shown in Figure 5(c), the rate constants based on TS3(w/ HB) are higher than those based on TS3(w/o HB) at low temperatures since the relative energy of TS3(w/ HB) is lower than that of TS3(w/o HB) by 4.0 kcal/mol. However, a good agreement of rate constants has been observed between the 1D-HR(w/o HB) and Mendes et al.'s [11], because TS3(w/o HB) was selected as the lowest energy conformer by Mendes et al. [11] in their calculations.

During the course of rate constant calculations, we found that the distinctly different low-frequency harmonic modes may cause large discrepancies of rate constants. Specifically, rate constants of R3 with TS3(w/ HB) remain much higher than that of R3 with TS3(w/o HB), if all the internal degrees of freedom were treated as harmonic oscillators (HO). This is because the B3LYP

functional generates a very loose structure for TS3(w/o HB) and thereby produces significantly small frequencies for a few harmonic modes in the structure, as seen in Table S4 of Supplementary Material IV. Furthermore, the uncertainty of frequency calculations was evaluated by employing two different theoretical methods, including the M06-2X and MP2 with the basis set of 6-311++G(d,p), which are expected to generate tighter structures and higher frequencies for low-frequency harmonic modes in TS3(w/o HB). As shown in Figure 6, the rate constants with the M06-2X and MP2 frequencies for low-frequency harmonic modes agree significantly better with those by the MS method.

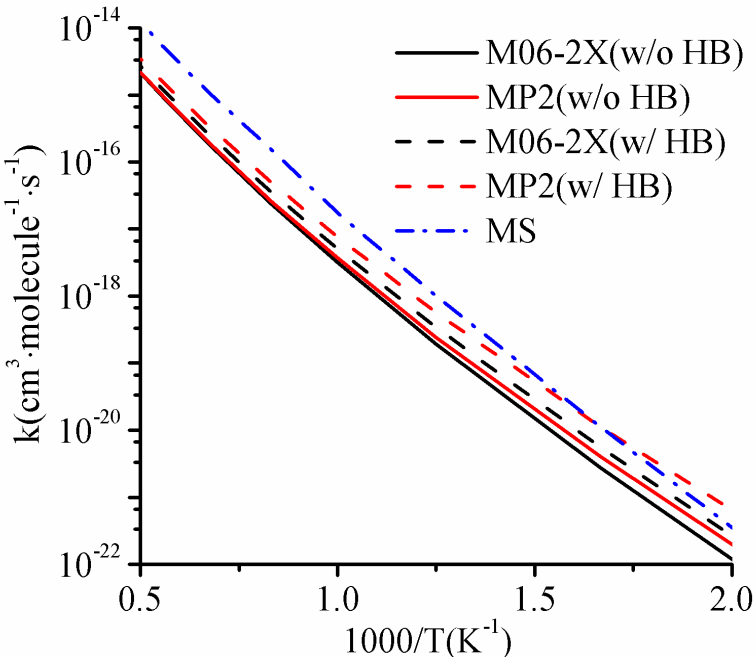

Figure 6. High-pressure rate constants for R3 by the 1D–HR and MS methods. M06-2X/6-311++G(d,p) and MP2/6-311++G(d,p) frequencies for low-frequency harmonic modes are used in the 1D-HR treatment

For R4 shown in Figure 5(d), the rate constants based on either TS4(w/ HB) or TS4(w/o HB) are close to each other and agree well with those of Mendes et al.[11]. However, these rate constants are smaller than those from the MS method by about one order of magnitude. As discussed in the preceding section, the large disagreement is due to the significantly larger "A-factor" of the MS prediction based on 88 conformational structures of TS4.

3.4 Influence of Addition Reaction

The multiple-well Master equation analysis of the PES shown in Figures 1-2 and S1-S3 confirms our assumption that the addition reaction leading to the formation of INT1 is kinetically dominant at sufficiently low temperatures because it has a significantly lower energy barrier compared with those of the abstraction reactions. However, an interesting "well merging" phenomenon emerges as temperature increases to above 300K, at which the reaction rate from INT1 to the reactants becomes comparable to the rate of its internal energy relaxation due to molecular collisions. As a result, INT1 cannot be treated as a kinetically distinguishable species above 300K. The detailed theoretical interpretation and mathematical formulation were given in previous studies [25, 31]. Specifically, R5 has an energy barrier of 5.0 kcal/mole to form the complex INT1 and the energy barrier of the reverse reaction is 4.95 kcal/mol, and therefore readily subject to the "well merging" phenomenon as temperature increases. The eigenvalues for the chemically significant eigenmodes (CSE) and a few of the lowest internal energy relaxation eigenmodes (IERE) [31-33] as functions of temperature at 1 atm and at 100 atm are shown in Figure 7 to illustrate the "well merging" phenomenon. At 1 atm, as temperature increases to about 300 K, CSE6, representing the addition reaction of HO2 to MB, merges with the IERE continuum, implying the "merging" of INT1 to reactants. The isomerization and decomposition reactions of INT1 are completely determined by the energy barriers of transition states of TS6, TS7, TS8, TS9, which are however much higher than those of the abstraction reactions. For the lowest energy barrier of the isomerization reaction is 21.4 kcal/mol, nearly 10 kcal/mol higher than that of R2, shown in Figure 1. Furthermore, the following energy barrier of decomposition reaction of INT6 is as large as 29.8 kcal/mol. As a result, the addition channel is not significant when the temperature is higher than 300 K. By increasing the pressure to about 100 atm, CSE6 merges with the IERE continuum at around 450 K, and the addition reaction is unimportant beyond the temperature.

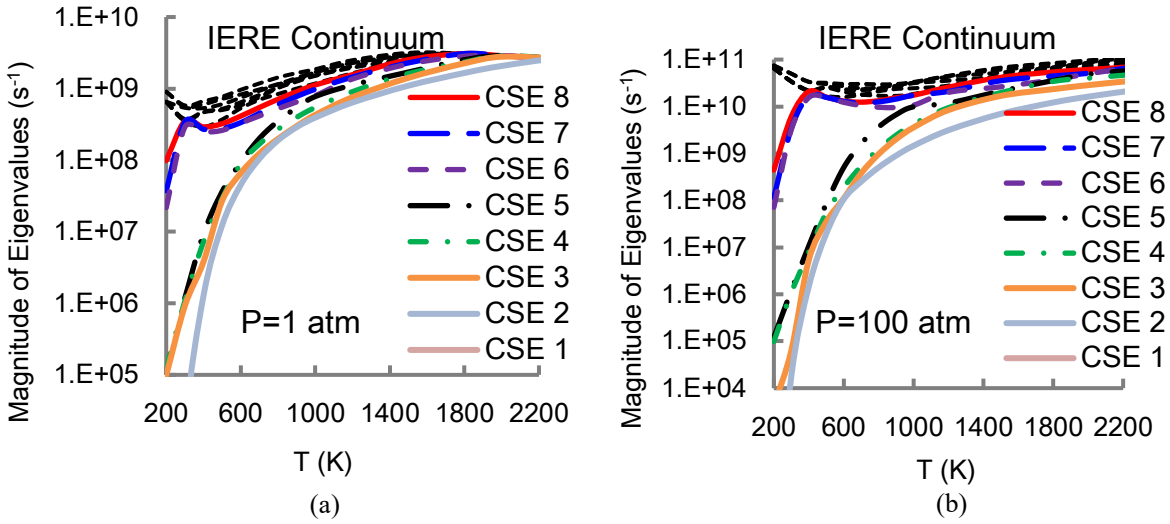

Figure 7. Chemically significant eigenvalues (CSEs) and internal energy relaxation eigenvalues (IEREs) for HO_2-addition reactions of MB+HO_2 as functions of temperature at (a) 1atm and (b) 100 atm.

3.5 Total Rate Constants of R1-R4

The total rate constants of R1–R4 are shown in Figure 8 and compared with previous results reported in the literature. The rate constants in the kinetic mechanism of MB by Dooley et al.[5] and Fisher et al.[6], and are significantly larger than the present predictions in the temperature range of 500K-1500K. In order to improve the agreement between computational and experimental results, Walton et al. [9] modified the rate constants in the kinetic mechanism of MB by Metcalfe et al.[8] by reducing the A-coefficients with a factor of 0.77, which overshoot the present predictions by a factor of 2 at lower temperatures while undershoot by the same factor at higher temperatures. Mendes et al.'s theoretical predictions are slightly higher than the present results below 800K while exhibit excellent agreement at higher temperatures[11].

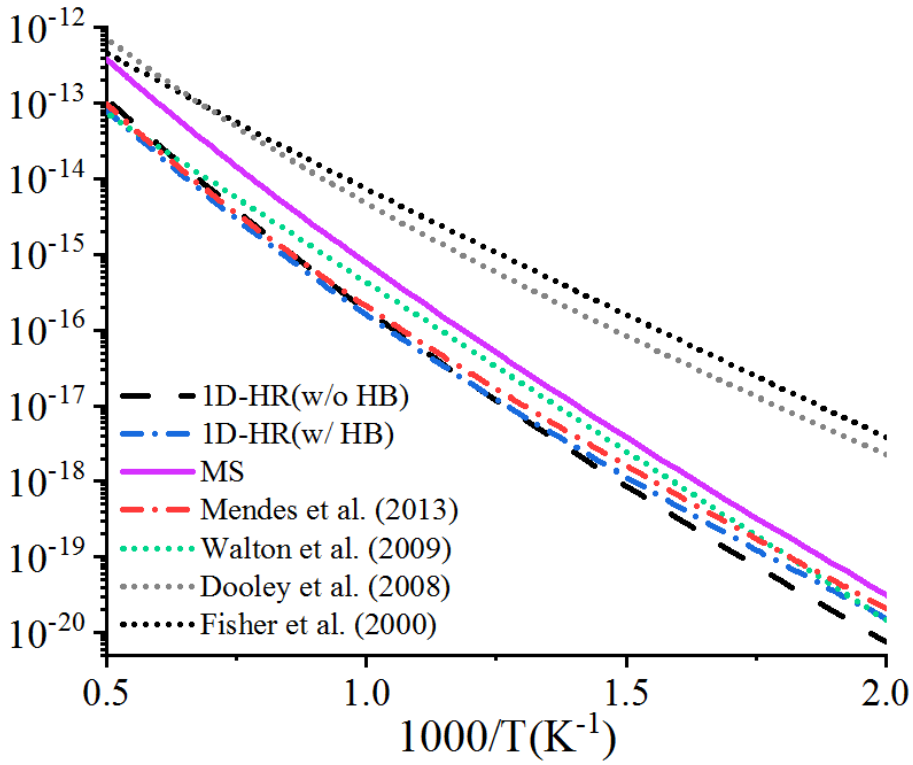

Figure 8. The high-pressure total reaction rates of the hydrogen abstraction reactions of MB+HO_2.

The present predictions for the total rate constants by the 1D–HR method are lower than those by the MS method, which is attributable to that the MS method may overestimate the rate constant of R3 and R4. Thus, we must be cautious to use it to validate the adequacy of the 1D–HR in dealing with torsional anharmonicity of complex systems. Although these two methods generate close rate constants for R1 and R2, they have discrepancies in rate predictions for R3 and R4. Further comparison is impossible without experimental data for each reaction.

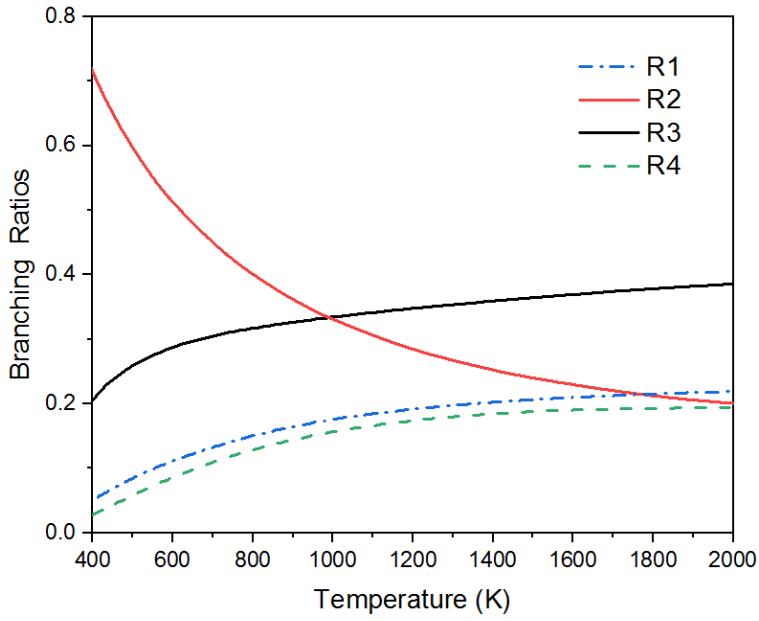

Figure 9. Branching ratios of abstraction reactions for MB + HO_2

As the addition reactions have no significant roles on determining the rate constants of MB + HO_2, only the branching ratios of abstraction reactions of MB + HO_2 were shown in Figure 9. It is noted that at low and medium temperature zone, the reaction leading to the MB3J is the most favorable due to the lowest energy barriers, and that forming the MB4J is the secondary. As temperature increases, the branching ratio of the MD3J formation decreases and then keeps steady. On the contrary, branching ratios of R1, R3 and R4 exhibits the positive temperature dependence and remain unchanged at high temperatures above 1000 K. At temperature high than 1500 K, the branching ratio of R1, R2, R3 and R4 are about 0.2, 0.2, 0.4 and 0.2, respectively, which is dominant by the similar entropy change, even though the energy barriers of these reactions differs largely with each other. Rate constants of the abstraction reactions of MB + HO_2 were summarized in Table 2, where it is fitting by using the Arrhenius equations.

Table 2. Calculated rate constants for R1-R4 reactions of MB+HO_2.k(T)=AT^nexp(-E/RT).

Reactions	A	n	E
MB + HO_2→MB2J + H_2O_2 (R1)	3.08	-3.02	39.24
MB + HO_2→MB3J + H_2O_2 (R2)	3.83	-3.16	36.06
MB + HO_2→MB4J + H_2O_2 (R3)	6.15	-3.07	38.07
MB + HO_2→MBMJ + H_2O_2 (R4)	0.99	-2.94	37.35

Units of k(T), A and E are $cm^3molecule^{-1}s^{-1}$, $cm^3molecule^{-1}s^{-1}$ and kcal/mol.

4. Concluding Remarks

All the possible reactions including the abstraction reactions and the addition reactions of MB and HO_2 were theoretically explored by the ab initio transition state theory based on multiple well master equation analysis. The results prove that the rate constants of MB + HO_2 are dominated by four hydrogen abstraction reactions at temperatures above 500K. The addition reaction channel leading to the formation of the complex INT1, which has the lowest energy barrier on the PESs of MB+HO_2, has a secondary contribution to the total rate of MB+HO_2, because of INT1 is readily decomposed back to the reactants at relatively low temperatures while the decompositions to other bimolecular products are not energetically favorable.

Structurally distinct and energetically similar torsional states of the transition states both with or without intramolecular hydrogen bonds were identified and considered in the rate calculations. TS (w/ HB) and TS (w/o HB) should be treated as distinguishing conformers, for the two configurations cannot be transferred to each other by only using the internal rotation, and the energy discrepancies can be as large as 4.0 kcal/mole. Generally, those TS conformers with hydrogen bond have lower energy than those without hydrogen bond, which brings about the rate constants of TS (w/ HB) are higher than those of TS (w/o HB) at low temperatures. At higher temperatures, the rate constants of TS (w/ HB) are close to those of TS (w/o HB).

The partition function of the transition states evaluated by using the MS method suggests the existence of strongly coupled internal rotation, which is absent in the conventional 1D hindered rotor approximation. The torsional anharmonicity treated by the MS method cause close (MB3J) or moderately higher (MB2J, MB4J) rate constants compared with that by the 1D-HR method, but it causes significantly higher rate constants for MBMJ due to the presence of a large number of low-energy conformers of the global minimum.

Regardless of the fact that the MS method exceeds theoretically the 1D–HR method, the significant amount of electronic structure calculations required by the former makes it too computational expensive to be a routine procedure in rate calculations. Consequently, future studies are merited for developing alternative and efficient approximate methods to supplement the widely-used 1D–HR method for accounting for torsional anharmonicity and coupling in complex molecular systems.

Acknowledgement

This work in the Hong Kong Polytechnic University was supported by Natural Science Foundation of China (91641105) and by the university matching fund (BCE8 and YBXN). The work in USTC was supported by Natural Science Foundation of China (51676176, 11575178 and U1532137).

Reference

[1].C. K. Westbrook; W. J. Pitz; H. J. Curran, Chemical kinetic modeling study of the effects of oxygenated hydrocarbons on soot emissions from diesel engines. *The Journal of Physical Chemistry A* **2006,** *110* (21), 6912-6922.
[2].J. Y. Lai; K. C. Lin; A. Violi, Biodiesel combustion: advances in chemical kinetic modeling. *Progress in Energy and Combustion Science* **2011,** *37* (1), 1-14.
[3].Q. Meng; Y. Chi; L. Zhang; P. Zhang; L. Sheng, Towards high-level theoretical studies of large biodiesel molecules: an ONIOM/RRKM/Master-equation approach to the isomerization and dissociation kinetics of methyl decanoate radicals. *Physical Chemistry Chemical Physics* **2019,** *21* (9), 5232-5242.
[4].Q. Meng; X. Zhao; L. Zhang; P. Zhang; L. Sheng, A theoretical kinetics study on low-temperature reactions of methyl acetate radicals with molecular oxygen. *Combustion and Flame* **2018,** *196*, 45-53.
[5].S. Dooley; H. J. Curran; J. M. Simmie, Autoignition measurements and a validated kinetic model for the biodiesel surrogate, methyl butanoate. *Combustion and Flame* **2008,** *153* (1), 2-32.
[6].E. M. Fisher; W. J. Pitz; H. J. Curran; C. K. Westbrook, Detailed chemical kinetic mechanisms for combustion of oxygenated fuels. *Proceedings of the combustion institute* **2000,** *28* (2), 1579-1586.
[7].S. Gaïl; M. J. Thomson; S. M. Sarathy; S. A. Syed; P. Dagaut; P. Diévart; A. J. Marchese; F. L. Dryer, A wide-ranging kinetic modeling study of methyl butanoate combustion. *Proceedings of the Combustion Institute* **2007,** *31* (1), 305-311.
[8].W. K. Metcalfe; S. Dooley; H. J. Curran; J. M. Simmie; A. M. El-Nahas; M. V. Navarro, Experimental and modeling study of C5H10O2 ethyl and methyl esters. *The Journal of Physical Chemistry A* **2007,** *111* (19), 4001-4014.

[9].S. M. Walton; M. S. Wooldridge; C. K. Westbrook, An experimental investigation of structural effects on the auto-ignition properties of two C5 esters. *Proceedings of the Combustion Institute* **2009,** *32* (1), 255-262.
[10]. W. Liu; R. Sivaramakrishnan; M. J. Davis; S. Som; D. E. Longman; T. F. Lu, Development of a reduced biodiesel surrogate model for compression ignition engine modeling. *Proc. Combust. Inst.* **2013,** *34* (1), 401-409.
[11]. J. Mendes; C. W. Zhou; H. J. Curran, Theoretical and kinetic study of the hydrogen atom abstraction reactions of esters with H(O.)2 radicals. *The journal of physical chemistry. A* **2013,** *117* (51), 14006-18.
[12]. L. Zhang; P. Zhang, Towards high-level theoretical studies of large biodiesel molecules: an ONIOM [QCISD (T)/CBS: DFT] study of hydrogen abstraction reactions of C n H 2n+ 1 COOC m H 2m+ 1+ H. *Phys. Chem. Chem. Phys.* **2015,** *17* (1), 200.
[13]. S. Le Calvé; G. Le Bras; A. Mellouki, Kinetic studies of OH reactions with a series of methyl esters. *The Journal of Physical Chemistry A* **1997,** *101* (48), 9137-9141.
[14]. X. Yang; D. Felsmann; N. Kurimoto; J. Krüger; T. Wada; T. Tan; E. A. Carter; K. Kohse-Höinghaus; Y. Ju, Kinetic studies of methyl acetate pyrolysis and oxidation in a flow reactor and a low-pressure flat flame using molecular-beam mass spectrometry. *Proceedings of the Combustion Institute* **2015,** *35* (1), 491-498.
[15]. S. J. Klippenstein; L. B. Harding; M. J. Davis; A. S. Tomlin; R. T. Skodje, Uncertainty driven theoretical kinetics studies for CH 3 OH ignition: HO 2+ CH 3 OH and O 2+ CH 3 OH. *Proceedings of the Combustion Institute* **2011,** *33* (1), 351-357.
[16]. P. Seal; E. Papajak; D. G. Truhlar, Kinetics of the Hydrogen Abstraction from Carbon-3 of 1-Butanol by Hydroperoxyl Radical: Multi-Structural Variational Transition-State Calculations of a Reaction with 262 Conformations of the Transition State. *The Journal of Physical Chemistry Letters* **2012,** *3* (2), 264-271.
[17]. J. Zheng; P. Seal; D. G. Truhlar, Role of conformational structures and torsional anharmonicity in controlling chemical reaction rates and relative yields: butanal + HO2reactions. *Chem. Sci.* **2013,** *4* (1), 200-212.
[18]. J. Zheng; D. G. Truhlar, Quantum Thermochemistry: Multistructural Method with Torsional Anharmonicity Based on a Coupled Torsional Potential. *Journal of Chemical Theory and Computation* **2013,** *9* (3), 1356-1367.
[19]. J. Zheng; T. Yu; E. Papajak; I. M. Alecu; S. L. Mielke; D. G. Truhlar, Practical methods for including torsional anharmonicity in thermochemical calculations on complex molecules: the internal-coordinate multi-structural approximation. *Physical chemistry chemical physics : PCCP* **2011,** *13* (23), 10885-907.
[20]. L. Simón-Carballido; J. L. Bao; T. V. Alves; R. Meana-Pañeda; D. G. Truhlar; A. Fernández-Ramos, Anharmonicity of Coupled Torsions: The Extended Two-Dimensional Torsion Method and Its Use To Assess More Approximate Methods. *Journal of Chemical Theory and Computation* **2017,** *13* (8), 3478-3492.
[21].A. Fernández-Ramos, Accurate treatment of two-dimensional non-separable hindered internal rotors. **2013,** *138* (13), 134112.
[22]. I. Alecu; J. Zheng; E. Papajak; T. Yu; D. G. Truhlar, Biofuel Combustion. Energetics and Kinetics of Hydrogen Abstraction from Carbon-1 in n-Butanol by the Hydroperoxyl Radical Calculated by Coupled Cluster and Density Functional Theories and Multistructural Variational Transition-State Theory with Multidimensional Tunneling. *The Journal of Physical Chemistry A* **2012,** *116* (50), 12206-12213.
[23]. R. Krishnan; J. S. Binkley; R. Seeger; J. A. Pople, Self-consistent molecular orbital methods. XX. A basis set for correlated wave functions. *The Journal of Chemical Physics* **1980,** *72* (1), 650. 成明
[24]. A. D. Becke, Density-functional thermochemistry. III. The role of exact exchange. *The Journal of Chemical Physics* **1993,** *98* (7), 5648.
[25]. P. Zhang; S. J. Klippenstein; C. K. Law, Ab initio kinetics for the decomposition of hydroxybutyl and butoxy radicals of n-butanol. *The journal of physical chemistry. A* **2013,** *117* (9), 1890-906.
[26]. M. Frisch; G. Trucks; H. Schlegel; G. Scuseria; M. Robb; J. Cheeseman; G. Scalmani; V. Barone; B. Mennucci; G. Petersson, Gaussian 09, revision A. 1. *Gaussian Inc., Wallingford, CT* **2009**.
[27]. C. Eckart, The penetration of a potential barrier by electrons. *Physical Review* **1930,** *35* (11), 1303.
[28]. C. Møller; M. S. Plesset, Note on an approximation treatment for many-electron systems. *Physical Review* **1934,** *46* (7), 618.V
[29]. A. L. East; L. Radom, Ab initio statistical thermodynamical models for the computation of third-law entropies. *The Journal of chemical physics* **1997,** *106* (16), 6655-6674.
[30]. L. Zhang; Q. Chen; P. Zhang, A theoretical kinetics study of the reactions of methylbutanoate with hydrogen and hydroxyl radicals. *Proc. Combust. Inst.* **2015,** *35* (1), 481.
[31]. A. Fernández-Ramos; J. A. Miller; S. J. Klippenstein; D. G. Truhlar, Modeling the kinetics of bimolecular reactions. *Chemical reviews* **2006,** *106* (11), 4518-4584.
[32]. J. A. Miller; S. J. Klippenstein, Master equation methods in gas phase chemical kinetics. *The Journal of Physical Chemistry A* **2006,** *110* (36), 10528-10544.
[33]. J. A. Miller; S. J. Klippenstein, Determining phenomenological rate coefficients from a time-dependent, multiple-well master equation:“species reduction” at high temperatures. *Physical Chemistry Chemical Physics* **2013,** *15* (13), 4744-4753.